Theory of spin-polarized angle-resolved photoemission spectroscopy of ferromagnetic nickel surfaces

A. Ishii, K. Yamada, and T. Aisaka
Department of Physics, Faculty of General Education, Tottori University, Koyama, Tottori 680, Japan

T. Kraft
Fritz-Haber-Institut der Max-Planck-Gesellschaft, Faradayweg 4-6, D-14195, Berlin, Germany
(Received 22 November 1993; revised manuscript received 22 June 1994)

A one-step model calculation of spin-polarized angle-resolved ultraviolet photoemission spectroscopy for ferromagnetic Ni(100), Ni(110), and Ni(111) is presented taking into account the band structure, electronic wave functions, and atomic configuration near and at the surface. The atomic structure and electronic potentials of the three nickel surfaces were determined from self-consistent full-potential linear muffin-tin orbital slab calculations. The calculated spin-polarized photoemission spectra show that the structural relaxation of the surface atomic layers plays a significant role.

I. INTRODUCTION

The electronic structure of ferromagnetic nickel has been studied experimentally and theoretically by a lot of works in the recent decade. The electronic band structure and the exchange splitting exhibit a small but noticeable discrepancy between band structure calculations and measured ARUPS (angle-resolved ultraviolet photoemission spectroscopy). The measured occupied band width and exchange splitting have been reported to be reduced by 30% and 50% from them for the bulk band calculation, respectively.[1-3]

The origin of the above disagreement is assigned to the incomplete treatment of electron correlation in the spin-polarized electronic system. Several theoretical studies addressed this problem, most of them employed a Hubbard model together with empirical parameter, and some apparently succeeded to explain the observed band structure.[4-12] We note, however, that there are very few many-body studies of electron correlation which are free of adjustable parameters. Some recent works[13-15] combined a first-principles band structure calculation taking into account nonlocal effect of exchange and correlation. When the theoretical results were compared to experiments he did, however, not take surface effect into account. This might be a severe neglect because band structure measurement done using ARUPS for which the analyzed electrons come mainly from surface region.

Therefore, it is still not clear whether the discrepancy between ARUPS experiments and bulk band calculations is not done using surface effect and the photoemission process. Therefore it is the purpose of this paper to present the calculations of ARUPS spectra for ferromagnetic nickel surfaces of realistic atomic structures and good quality electronic potential in order to analyze the electrons of the surface. We performed self-consistent spin-polarized full-potential linear muffin-tin orbital (FP-LMTO) calculations for slabs of Ni(100), Ni(110), and Ni(111) to determine the surface atomic configuration and to obtain spin-polarized effective potentials. This is done by using density-functional theory together with the local-spin density approximation for the exchange-correlation functional. We then make spherical muffin-tin potentials and calculate photoemission spectra using the one-step model[16] in the formulation of multiple-scattering calculation scheme.

II. CALCULATION SCHEME TO DETERMINE ATOMIC STRUCTURE

The calculations described below consist of two parts: (i) making self-consistent muffin-tin-potentials for the surface layers, and (ii) calculating ARUPS. To construct muffin-tin potentials for nickel atoms in the topmost several surface layers, we employ density-functional theory together with the FP-LMTO method.[17-20] The basis set consists of atom-centered s,p, and d orbitals, each of them with three different radial function (augmented Hankel function). The method allows for a correct treatment of nonspherical terms in the charge density and the potential. We use the local spin-density approximation of the exchange-correlation functional.[21,22] The $\mathbf{k}$ space sampling was done on a uniform mesh of 35 $\mathbf{k}$ points in the irreducible wedge of the surface Brillouin zone. To model the Ni(100) surface we take a nine-layer slabs and for Ni(110) and (111) the slabs consisted of ten and eleven layers. The two top surface layers are allowed to relax perpendicular to the surface in order to minimize the total energy. The muffin-tin potentials needed for the photoemission calculations are obtained by evaluating the spherical arrangement of the FP-LMTO potentials. The atoms of the topmost four atomic layers have muffin-tin potentials which are different from the bulk one.

For ARUPS calculation, we use the program code, NEWPOOL.[23] In the one-step model of photoemission,[16] the photocurrent is presented as the following equation,

$$I(\omega,\mathbf{k})=\int\int d\mathbf{r}\,d\mathbf{r}'\Psi_{\mathbf{k}}^{*}(\mathbf{r},E+\hbar\omega)\Delta(\mathbf{r})G(\mathbf{r},\mathbf{r}',E)\Delta(\mathbf{r}')\Psi_{\mathbf{k}}(\mathbf{r}',E+\hbar\omega)\ , \tag{1}$$

where $\Psi_{\mathbf{k}}(\mathbf{r}',E+\hbar\omega)$ is the wave function of the emitted photoelectron with energy $E+\hbar\omega$ and momentum $\mathbf{k}$, $G(\mathbf{r},\mathbf{r}',E)$ is the Green function of an electron of the target nickel crystal, and $\Delta(\mathbf{r})$ is the photoexcitation coupling term,

$$\Delta(\mathbf{r})=\frac{\mathbf{A}\cdot\nabla V}{\hbar\omega c}\ , \tag{2}$$

where V is the effective potential for the electron and c is light velocity. The electronic wave function and Green functions are calculated within the layer-KKR scheme.[24] Since the calculation scheme for the photoelectron wave function, $\Psi_{\mathbf{k}}(\mathbf{r}',E+\hbar\omega)$, is identical to that of low-energy electron diffraction (LEED), it is to be expected that the calculated photocurrent $I(\hbar\omega,\mathbf{k})$ is sensitive to the surface atomic configurations. In the present calculation, we consider a 1×1 surface structure in agreement with the LEED patterns observed for the studied surface. Thus, there is no surface reconstruction, but we take into account that the topmost two atomic layers have different spacings than the bulk. The surface barrier potential is approximated by a simple steplike function.

We also use the Green function KKR program,[25] to obtain the local density of states for each layer. This calculation is based on the same concept and practically the same methods as the photoemission program.

III. RESULT

A. Ni(100)

According to the self-consistent spin-polarized full-potential LMTO calculation for a nine-layer slab of Ni(100) surface, we obtain after energy minimization that the topmost layer has -3% relaxation and the second layer has $+1.2\%$ relaxation. The result is comparable to the LEED analysis[26] where the topmost layer has been observed to be contracted.

In Figs. 1 and 2, we show the local density of states (DOS) of Ni(100) at $\bar{\Gamma}$ point for the topmost four surface layers by using the Moruzzi-Janak-Williams (MJW)[27] spin-polarized muffin-tin potentials. The local DOS's for the ideal Ni(100) crystal face (no relaxation) are shown in Fig. 1 where the solid and the dashed lines correspond to the majority and minority spin. In Fig. 2, the topmost layer has 3% contraction and the second outermost layer has 1.2% relaxation which are taken to be the same as the self-consistent full-potential LMTO calculation above. The original self-consistent LMTO potentials are almost spherical that the spherically symmetric muffin-tin potential is considered to be a very good approximation.

From Fig. 1, we first found some general features of surface local density of states. The topmost two layers have the distinct local DOS profiles from the deeper layers both for the majority and minority spin. The profile of the local DOS of the topmost layer is smeared out in comparison with that of the bulk layer. The profiles for the outermost layer are especially different from the others. It should be pointed out strongly that such features would be also quite important in the case of analysis of scanning tunnel microscope images or scanning tunneling spectroscopy spectra. Since the ultraviolet photoemission is also a surface-local phenomenon because of the short mean-free path for the emitted photoelectron,[28] The distinct features of the topmost few layers are dominant to the ARUPS spectrum. Thus, we can easily expect that the surface structure of the target is very important to analyze ARUPS experiment. We should also mention that the exchange splitting itself looks the same for these four layers.

In Fig. 2, we found the effect of the surface relaxation of the atomic structure. The local DOS curves of the topmost three layers seem clearly different from those of Fig. 1. Thus, even for a few percent, the surface relaxation effect is not negligible for the local DOS of surface electrons. For the fourth layer, the profile of Figs. 1 and 2 looks similar, however. It is considered that the electronic property of the fourth layer is almost bulklike.

In Fig. 3, we show the calculated local DOS due to the self-consistent full-potential LMTO method. According to the slab calculation above, we take -3% relaxation for the topmost layer and $+1.2\%$ relaxation for the second layer. The spin-polarized ferromagnetic muffin-tin potentials of nickel atoms in the topmost four layers are different from the bulk layer. Thus, we use five different nickel potentials for both majority and minority nickel atoms in the local DOS calculation. The results in Fig. 3 are quite different from those in Figs. 1 and 2, especially for the outermost layer. In Fig. 4, we show three local DOS curves on the topmost layer for three different calculation schemes: ideal crystal with the MJW poten-

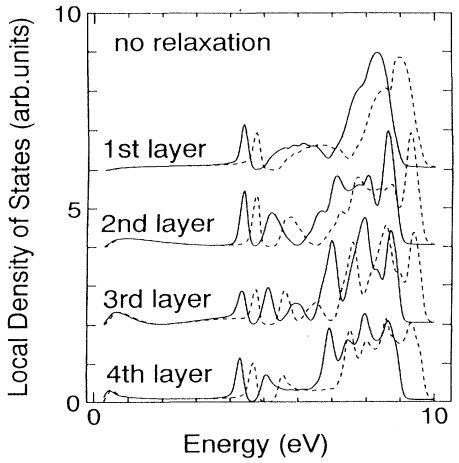

FIG. 1. Calculated local density of states for electron of Ni(100) surface with ideal crystal structure and bulk potential of Moruzzi, Janak, and Williams. The energy is measured from the muffin-tin-zero $\bar{\Gamma}$ point. The solid lines are for electron having majority spin and dashed lines are for electron having minority spin.

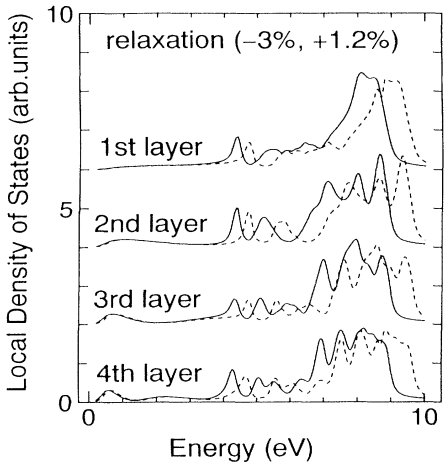

FIG. 2. Calculated local density of states for electron of Ni(100) surface with relaxation of the topmost two layers indicated in the figure and bulk potential of Moruzzi, Janak, and Williams. The energy is measured from the muffin-tin-zero $\bar{\Gamma}$ point. The solid lines are for electron having majority spin and dashed lines are for electron having minority spin.

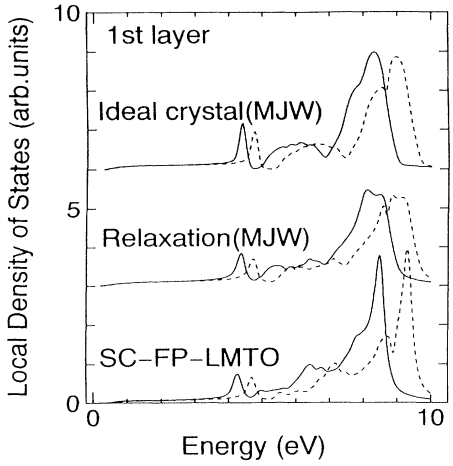

FIG. 4. Comparison of the three calculated local density of states for electron of Ni(100) surface for the topmost layer. The energy is measured from the muffin-tin-zero $\bar{\Gamma}$ point. The solid lines are for electron having majority spin and dashed lines are for electron having minority spin.

tial, relaxation with the MJW potential, and the self-consistent full-potential LMTO calculation. It is distinctly observed that the curve due to FP-LMTO is completely different from the other two that are rather similar. Nevertheless, the exchange-splitting value seems the same for three of the curves. The significant conclusion from this figure is that the self-consistent calculation for the surface electronic system is very important to calculate the local DOS which is usually different from the bulk local DOS. In Fig. 5, we show a similar figure for the fourth layer. As we expected, the three curves are very similar. It means that the self-consistent calculation is extremely important only for the surface region. For the bulk electronic property, the self-consistent calculation would be less significant than the surface system.

In Figs. 6 and 7, we show the ARUPS spectra for the relaxation surface with the bulk potential and for the relaxation surface with the self-consistent potentials. According to the experiment of Mårtensson and Nilsson,[29] we choose the condition that the incident photon energy is $\hbar\omega = 21.22$ eV, incident angle is 30°, and normal emission. Since the incident light is unpolarized, *s*- and *p*-polarized light are mixed together on a fifty-fifty basis. The imaginary part of the electronic energy for photoelectron is 4.0 eV and for surface electron it is 0.14 eV.

In Fig. 6, we show calculated ARUPS spectra for ideal

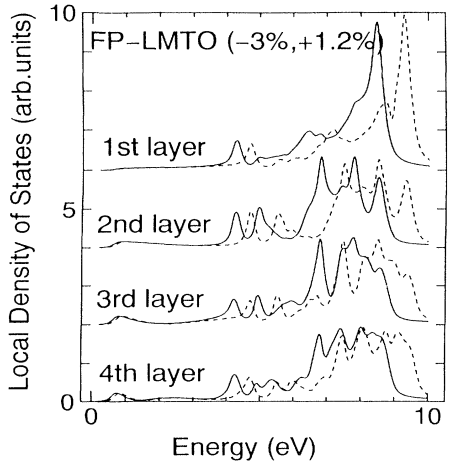

FIG. 3. Calculated local density of states for electron of Ni(100) surface with relaxation of the topmost two layers indicated in the figure and potentials consisted by full-potential LMTO formalism. The energy is measured from the muffin-tin-zero $\bar{\Gamma}$ point. The solid lines are for electron having majority spin and dashed lines are for electron having minority spin.

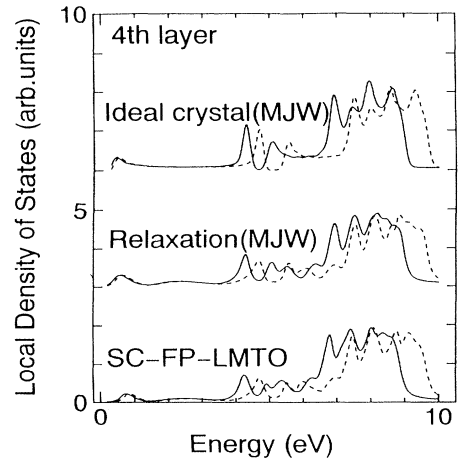

FIG. 5. Comparison of the three calculated local density of states for electron of Ni(100) surface for the fourth layer. The energy is measured from the muffin-tin-zero $\bar{\Gamma}$ point. The solid lines are for electron having majority spin and dashed lines are for electron having minority spin.

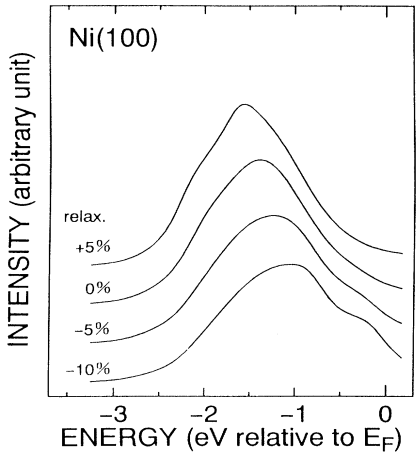

FIG. 6. Calculated ARUPS spectra for Ni(100) surface with various relaxation of the topmost atomic layer using the bulk potential of Moruzzi, Janak, and Williams. The incident photon energy, incident angle, and emission direction are 21.22 eV, 30°, and normal, respectively.

and relaxed structure Ni(100) with the MJW potential. Compared it with the experimental data (we can see it in Fig. 7), we could not get a fine agreement of even more than -10% relaxation. We should mention that the difference we see in Fig. 6 is larger than the difference in the local density of states, for example, in Fig. 4.

In Fig. 7, we show the calculated ARUPS spectra for the relaxed structure of -3% on the first and of $+1.2\%$ on the second layer spacing with the self-consistent full-potential LMTO potential. In contrast to Fig. 6, we found a very good agreement between the experiment and the computational result in Fig. 7. Moreover, from the spin-resolved data, we found that the peak positions of the majority and the minority spectrum do not correspond to the peak or shoulder of the total spectrum. Thus, if the spin-resolved ARUPS experiment is very difficult just like this case, the computational method to reproduce ARUPS spectra directly is a very useful method.

In Fig. 8, we show the difference of calculated ARUPS spectra with the self-consistent full-potential LMTO potential and the MJW potential for various photon energies. The result can be compared with the experiment of Ref. 25 and we find that our LMTO calculation agrees with them better.

In Fig. 9, we show the similar comparison for various emission angles with the incident energy of 21.22 eV which is again able to compare with the experimental data of Ref. 25. The calculation with the self-consistent full-potential LMTO shows better agreement with the experiment.

B. Ni(110)

Since there is experimental data of spin-resolved ARUPS[30] for Ni(110), this surface is one of the most important examples to investigate ferromagnetic band structure of transition metals. It is well known that the observed electronic level near the Fermi energy E_F is about half in comparison with theoretical band structures as we mentioned in the Introduction, if we measure electronic energy from E_F. At the moment, there are no theoretical calculations which can explain the above gap between the experiment and theory without introducing adjusting parameters.

We should point out strongly that no theoretical calculations have included surface effect, especially surface relaxation effect. However, surface relaxation of atomic layers has been reported on Ni(110), as we found in experimental works of LEED analysis. According to our result of Ni(100), we can easily imagine that such surface relaxation would moderate ARUPS spectrum a lot.

First, we show typical data of surface relaxation effect.

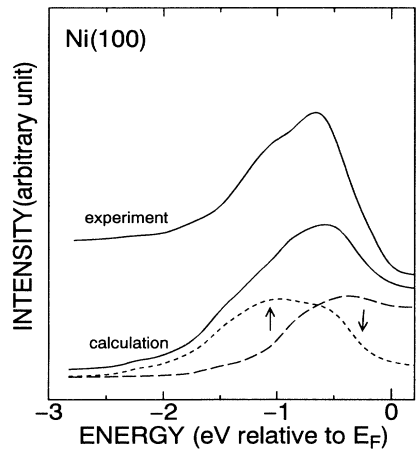

FIG. 7. Calculated ARUPS spectra for Ni(100) surface with the derived relaxation using potentials obtained by self-consistent full-potential LMTO calculation. The incident photon energy, incident angle, and emission direction are 21.22 eV, 30°, and normal, respectively.

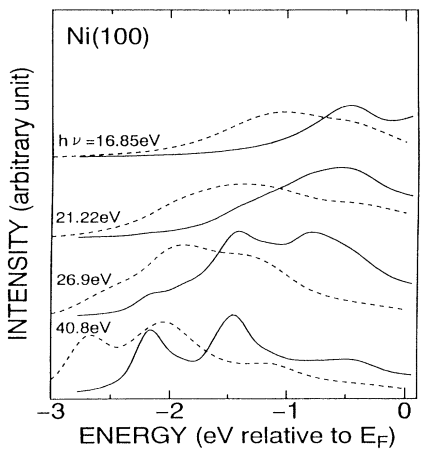

FIG. 8. Calculated ARUPS spectra for Ni(100) surface with various photon energy. The solid lines are for using potentials obtained by self-consistent full-potential LMTO calculation and dashed lines are for using bulk potential. The incident angle and emission direction are 45° and normal, respectively.

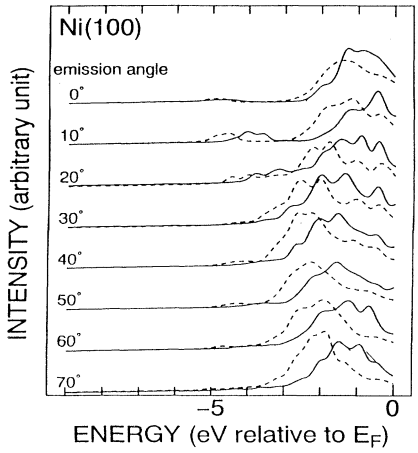

FIG. 9. Calculated ARUPS spectra for Ni(100) surface with various emission direction. The solid lines are for using potentials obtained by self-consistent full-potential LMTO calculation and dashed lines for using bulk potential. The incident photon energy and incident angle are 21.22 eV and 45°, respectively.

In Fig. 10, we show the calculation of spin-integrated ARUPS of Ni(110) for various surface relaxation case, where we take the bulk potential of nickel atom presented by Moruzzi, Janak, and Williams.[27] The calculated spectra are for normal emission with incident photon energy of 16.85 eV and incident angle of 30° according to the related experimental data. In the calculation, the relaxation of the layer spacing between the topmost and the second layer is taken into account. As we see in the figure, the calculated ARUPS spectrum is very sensitive to the surface relaxation, also for Ni(110). Especially, we should mention that the peak positions are sensitive to the relaxation of the topmost layer. Thus, it is concluded that, not only the electron correlation effect, but also the surface relaxation is a very significant factor to consider the quantitative agreement between theory and experiment for ARUPS. However, since the observed peaks in the experiment are located at −0.24 eV for majority and −0.06 eV for minority spin, the quantitative agreement between the observed peak positions and our calculation in Fig. 10 is not enough. We should notice that it is very difficult to obtain the calculated peak positions similar to the experiment, because even the surface relaxation of −15% is unrealistically large. Although the mean-free path of the electron and photoelectron are sometimes important factors to change the calculated spectrum, we confirmed that the moderation is not strong to change the location of the peak in the spectra.

Therefore, we proceed to the next calculation: ARUPS spectrum calculation with the muffin-tin potentials which are obtained from the self-consistent calculation by the full-potential LMTO, as we did for Ni(100). First, we perform the spin-resolved self-consistent calculation with a repeated slab of eleven layers. In the calculation, the topmost two layers of both sides are treated as relaxed atomic layers. The layer spacing among the central seven layers are fixed to be the bulk data. According to the calculation, we obtain the layer spacing between the topmost and the second atomic layer to be 9% contraction and the spacing between the second and the third layer is 3.5% relaxation. The obtained Fermi energy is 7.767 eV from the muffin-tin-zero level.

In Fig. 11, we show the calculated spin-resolved ARUPS spectrum due to the relaxed atomic structure and the muffin-tin potential obtained from the self-consistent full-potential LMTO. In comparison with Fig. 8, the peak position seems to be closer to the experimental value. In Table I, we collect the peak values we obtain from Figs. 10, 11, and the related experimental data. The "bulk calc." cited in the table comes from the band calculation of Moruzzi, Janak, and William.[27] As we see

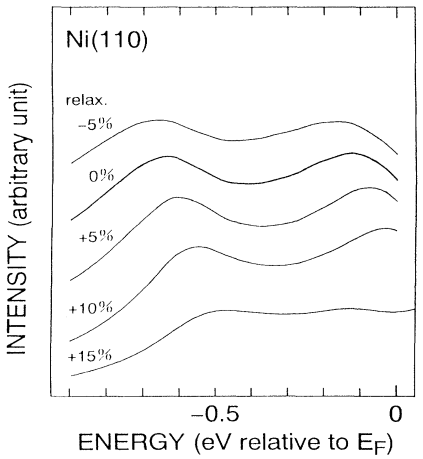

FIG. 10. Calculated ARUPS spectra for Ni(110) surface with various relaxation of the topmost atomic layer spacing using the bulk potential of Moruzzi, Janak, and Williams. The incident photon energy, incident angle, and emission direction are 16.85 eV, 30°, and normal, respectively.

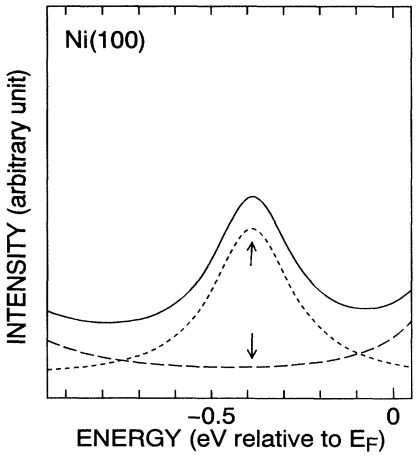

FIG. 11. Calculated ARUPS spectra for Ni(110) surface with the derived relaxation using potentials obtained by self-consistent full-potential LMTO calculation. The incident photon energy, incident angle, and emission direction are 16.85 eV, 30°, and normal, respectively.

TABLE I. Comparison of calculated peak position of Ni(110) spectra with experimental data. For MJW, surface relaxation between first and second layers is −10%. For self-consistent FP-LMTO, surface relaxation between first and second atomic layers is −9% and that between second and third atomic layers is +3.5%.

	up (eV)	down (eV)	splitting (eV)
Calc. (MJW)	−0.55	−0.02	0.53
Calc. (FP-LMTO)	−0.38	0	0.38
Band calc.	−0.465	0.095	0.56
Expt.	−0.24	−0.06	0.18

clearly in Fig. 11, our calculated peak for the minority spin state is located beyond the Fermi energy. Because of the sharp cut-off at the Fermi level and the finite resolution in the experimental spectra, it is quite possible that the sharp cut-off edge of the spectrum looks like a peak. Thus, we could conclude that the exchange-splitting value measured in the experiment of Hopster *et al.*[30] would not be the real exchange-splitting value: the peak of the minority spin state in the experiment would be just the sharp Fermi cut-off edge.

In Fig. 12, we show another calculation for inverse photoemission experiment from Donath *et al.*[31] The calculation with the self-consistent full-potential LMTO agrees far better than that with the bulk potential of MJW. A peak of the self-consistent full-potential LMTO spectra very near to the Fermi edge would be smeared out in the observation in the experiment. In Fig. 13, we show the spin-resolved inverse photoemission spectrum of the self-consistent full-potential LMTO version for the same experiment. We can expect that the peak of the up-spin electron near the Fermi level would be smeared out in the experimental measurement.

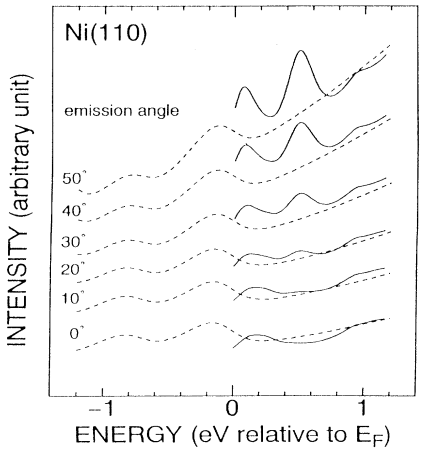

FIG. 12. Calculated inverse photoelectron spectra for Ni(110) surface with various emission direction. The solid lines are for using potentials obtained by self-consistent full-potential LMTO calculation and dashed lines for four using bulk potential. The incident electron energy and incident angle are 9.4 eV and 25°, respectively.

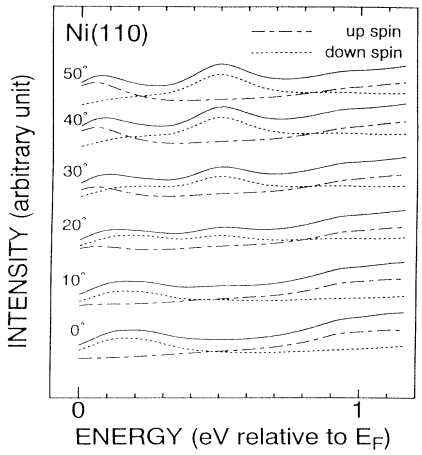

FIG. 13. Spin-resolved calculated inverse photoelectron spectra for Ni(110) surface with various emission direction. The dash-dotted and the dotted lines correspond to the majority and the minority spin spectrum using potentials obtained by self-consistent full-potential LMTO calculation. The solid lines are for the sum of the up spin and the down spin. The experiment condition is the same as that of Fig. 12.

C. Ni(111)

At last, we calculate the spin-resolved ARUPS spectra of Ni(111) surface. According to the self-consistent full-potential LMTO calculation for a repeated slab of nine layers similar to that for Ni(100) or Ni(110) above, we obtain that this surface has no surface relaxation. This result agrees with the LEED analysis.[32] As the muffin-tin potential for the ARUPS calculation below, the electronic potential for the atom of the centered layer is considered as a bulk muffin-tin potential and the potentials for that of the topmost four layers are different from the bulk one.

In Fig. 14, we show the calculated ARUPS spectra due to the bulk muffin-tin potential of Moruzzi, Janak, and Williams and then due to the self-consistent calculation. The experimental data[29] in the figure are obtained by the incident light energy of 21.22 eV, and incident angle of 45°. The light source is unpolarized and the detection is normal emission. In Fig. 15, we show the difference of the two calculated ARUPS spectra for various emission angles which we are able to compare with the experiment of Fig. 2 of Ref. 25. Moreover, in Fig. 16, we show our calculation for various photon energies which corresponds to the experiment of Kämper, Schmitt, and Güntherodt *et al.*[33] Again, we confirm that we obtain the far better result with the self-consistent potential. We conclude from Figs. 14–16 that even if there are no surface relaxation, the self-consistent atomic potential at surface is very important for ARUPS calculation.

IV. DISCUSSION

We can confirm several points of the surface effects in ARUPS calculation. There are two important surface effects: surface relaxation and electronic potential for

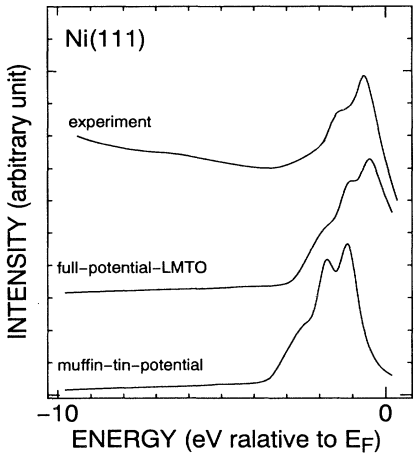

FIG. 14. Comparison of the experimental data, calculated ARUPS spectra for Ni(111) surface with the just-fit relaxation using the bulk potential (MJW), and with the derived relaxation using potentials obtained by self-consistent full-potential LMTO calculation. The incident photon energy, incident angle, and emission direction are 21.22 eV, 45°, and normal, respectively.

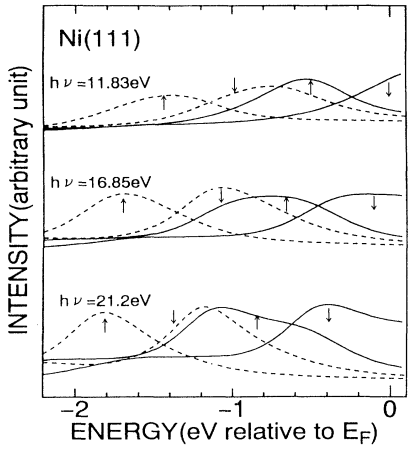

FIG. 16. Calculated ARUPS spectra for Ni(111) surface with various photon energy. The solid lines are for using potentials obtained by self-consistent full-potential LMTO calculation and dashed lines are for using bulk potential. The incident angle and emission direction are 30° and normal, respectively. ↑:majority-sin electrons; ↓:minority-spin electrons.

atoms of surface layers. The less important surface effect is the mean-free path of photoelectron and electron of an occupied level.

We found in Fig. 2 how significant is the inclusion of surface relaxation into the local DOS calculation. Though the exchange splitting value looks the same for the results with and without relaxation, the local LDOS curves seem to be clearly different from those of the ideal surface. In Fig. 6, we found the importance of the surface relaxation in ARUPS calculation. The most important conclusion in Fig. 6 is that the peak of ARUPS curves can be changed owing to the relaxation of surface atomic layer. According to the above calculations, we confirm that the surface relaxation of the target surface

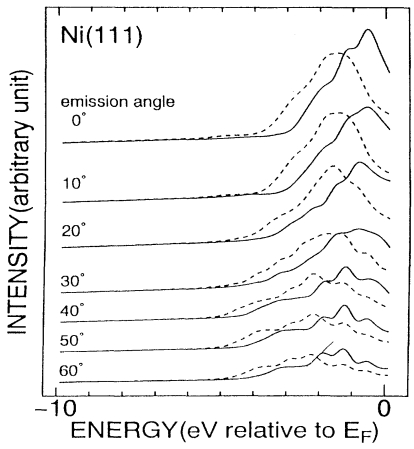

FIG. 15. Calculated ARUPS spectra for Ni(111) surface with various emission direction. The solid lines are for using potentials obtained by self-consistent full-potential LMTO calculation and dashed lines are for using bulk potential. The incident photon energy and incident angle are 21.22 ev and 45°, respectively.

should be taken into account for the quantitative discussion of the measurement of the band structure which is usually observed as peaks in ARUPS curves in various emission directions. Therefore, as a conclusion, we point out that experimentalists should take into account the surface relaxation of the target atomic structure when they measure ARUPS spectra; band structures measured with ARUPS are by no means bulk band structure. This conclusion is not only for ferromagnetic surface but for any ARUPS measurements.

The second significant conclusion we should point out from the above calculation is the importance of electronic potentials of atoms in surface atomic layers. The clear evidence of the importance is found in Fig. 14. In Fig. 14, the only difference in the actual calculation is whether or not we use the self-consistent potentials. In the self-consistent calculation, the nickel atoms in the topmost four layer are different from the bulk potential. Even though we did not include surface relaxation into the calculation, the difference of the two spectra in Fig. 14 is large. Moreover, we can easily conclude that the calculation with self-consistent potentials is better. Thus, the joint calculation of ARUPS spectrum with self-consistent electronic structure calculation is very useful for the quantitative discussion of the electronic structure.

In Figs. 7 and 9, we confirm that the calculated ARUPS s ectra with the effect of surface relaxation and the difference of electronic potentials in surface atomic layers agree far better with the experiments than the bulklike ARUPS spectrum calculation. From Figs. 7, 9, and 10, we obtain far better peak position than the ordinary bulk calculations to compare with the experimental value. Therefore, we conclude that one of the dominant factors of the disagreement between the measured and calculated band structures is the absence of the surface effects.

According to a lot of theoretical works, the electronic

correlation problem from the point of view of many-body theory has been pointed out to be important. However, every many-body theory has some adjusting parameters which are usually determined from the first principles. Thus, according to the present work, many-body theorists should consider the justification of the parameters after they include the surface effects. We obtain for Ni(110) that about 50% of the disagreement between experiment and theory with respect to the main band can be explained with the surface effects.

We should also point out that the exchange-splitting value itself is not sensitive to the surface effects. As we saw in Fig. 9, the position of the minority band relative to E_F is significant for the Ni(110) band structure measurement. The origin of the reduced exchange-splitting value is that they observe the Fermi edge instead of the minority band peak in the relative experiment.

V. CONCLUSION

We demonstrated that computationally surface effects appeared in spin-polarized ARUPS spectrum of ferromagnetic Ni(100), Ni(110), and Ni(111) clean surfaces with muffin-tin potentials which were due to slab calculation of self-consistent spin-polarized full-potential linear muffin-tin orbital formalism. The results agree better with experiments than previous bulk band calculations though complicated electron correlation is ignored. Thus, we can conclude that the consideration of the surface sensitivity with electron correlations are important to explain ferromagnetic nickel band structures. Therefore, the results show us that modification of electronic potentials for surface atoms and surface relaxation of atomic layer spacing are very significant in discussing quantitatively electronic band structures measured with ARUPS technique.

ACKNOWLEDGMENTS

All of the authors thank Professor M. Scheffler for his kind advice, especially for his idea to join the self-consistent FP-LMTO calculation with surface-sensitive ARUPS calculation. One of the authors (A.I.) is grateful for the Alexander von Humboldt foundation to give him an opportunity to make this joint research in the Fritz-Haber-Institute of the Max-Planck Society at Berlin. The authors in Japan acknowledge the support of the Grant-in-Aid of the Ministry of Education and Culture of Japan: Computational Solid State Physics. The authors are also grateful for the Computer Center of the Institute for Molecular Science at Okazaki, Japan.

[1]W. Eberhardt and E. W. Plummer, Phys. Rev. B **21**, 3245 (1980).
[2]D. E. Eastman, F. J. Himpsel, and J. A. Knapp, Phys. Rev. Lett. **40**, 1514 (1978).
[3]F. J. Himpsel, J. A. Knapp, and D. E. Eastman, Phys. Rev. B **19**, 2919 (1979).
[4]L. C. Davis and L. A. Feldkamp, Solid State Commun. **34**, 141 (1980).
[5]A. Liebsch, Phys. Rev. B **23**, 5203 (1981).
[6]G. Treglia, F. Ducastelle, and D. Spanjaard, J. Phys. (Paris) **43**, 341 (1982).
[7]R. Clauberg, Phys. Rev. B **28**, 2561 (1983).
[8]T. Aisaka, T. Kato, and E. Haga, J. Phys. F **14**, 2537 (1984).
[9]T. Aisaka, T. Kato, and E. Haga, Physica B **149**, 181 (1988).
[10]W. Nolting, W. Borgiel, V. Sode, and Th. Fauster, Phys. Rev. B **40**, 5015 (1989).
[11]C. Calandra and F. Manghi, Phys. Rev. B **45**, 5819 (1992).
[12]M. M. Steiner, R. C. Albers, and L. Sham, Phys. Rev. B **45**, 13 272 (1992).
[13]F. Aryasetiawan, Phys. Rev. B **46**, 13 051 (1992).
[14]M. A. Hoyland and R. G. Jordan, J. Phys. Condens. Matter **3**, 1337 (1991).
[15]J. Braun, W. Nolting, and G. Borstel, Surf. Sci. **251/252**, 22 (1991).
[16]J. B. Pendry, Surf. Sci. **57**, 679 (1976).
[17]M. Methfessel, Phys. Rev. B **38**, 1537 (1988).
[18]M. Methfessel, C. O. Rodriguez, and O. K. Andersen, Phys. Rev. B **40**, 2009 (1989).
[19]T. Kraft, P. M. Marcus, and M. Scheffler, Phys. Rev. B **49**, 11 511 (1994).
[20]T. Kraft, M. Methfessel, M. van Schlifgaarde, and M. Scheffler, Phys. Rev. B **47**, 9862 (1993).
[21]D. M. Ceperley and B. J. Alder, Phys. Rev. Lett. **45**, 566 (1980).
[22]S. H. Vosko, L. Wilk, and M. Nusair, Can. J. Phys. **58**, 1200 (1980).
[23]J. F. L. Hopkinson, J. B. Pendry, and D. Titterington, Computer Phys. Commun. **19**, 69 (1980).
[24]K. Kambe, Z. Naturforschg. **22a**, 422 (1966); **22a**, 322 (1966); **23a**, 1280 (1968).
[25]B. Wenzien, J. Bormet, and M. Scheffler (unpublished).
[26]J. W. M. Frenken, J. V. van der Veen, and G. Allan, Phys. Rev. Lett. **51**, 1876 (1983).
[27]V. L. Moruzzi, J. F. Janak, and A. R. Williams, *Calculated Electronic Properties of Metals* (Pergamon, New York, 1978).
[28]A. Ishii and T. Aisaka, Surf. Sci. **242**, 250 (1991).
[29]H. Mårtensson and P. O. Nilsson, Phys. Rev. B **30**, 3047 (1984).
[30]H. Hopster, R. Raue, G. Guntherodt, E. Kisker, R. Clauberg, and M. Campagna, Phys. Rev. Lett. **51**, 829 (1983).
[31]M. Donath, V. Dose, K. Ertl, and U. Kolac, Phys. Rev. B **41**, 5509 (1990).
[32]J. E. Demuth, P. M. Marcus, and D. W. Jepsen, Phys. Rev. B **11**, 1460 (1975).
[33]K.-P. Kämper, W. Schmitt, and G. Güntherodt, Phys. Rev. B **42**, 10 696 (1990).